EXISTENCE AND STABILITY ANALYSIS OF SPIKY SOLUTIONS FOR THE GIERER-MEINHARDT SYSTEM WITH LARGE REACTION RATES

THEODORE KOLOKOLNIKOV, JUNCHENG WEI, AND MATTHIAS WINTER

Abstract. We study the Gierer-Meinhardt system in one dimension in the limit of **large reaction rates**. First we construct three types of solutions: (i) an interior spike; (ii) a boundary spike and (iii) two boundary spikes. Second we prove results on their stability. It is found that an interior spike is always unstable; a boundary spike is always stable. The two boundary spike configuration can be either stable or unstable, depending on the parameters. We fully classify the stability in this case. We characterize the destabilizing eigenfunctions in all cases. Numerical simulations are shown which are in full agreement with the analytical results.

1. Introduction

In this paper, we study the Gierer-Meinhardt system in the limit of **large reaction rates**. Let us first put it in the context of Turing's diffusion-driven instability. Since the work of Turing [16] in 1952, many models have been established and investigated to explore the so-called Turing instability [10]. One of the most famous models in biological pattern formation is the Gierer-Meinhardt system [4], [8], [9], which in one dimension can be stated as follows:

$$\begin{aligned} &A_t = D_A \Delta A - A + \frac{A^p}{H^q}, \quad x \in (-1,1),\ t>0, \\ &\tau H_t = D_H \Delta H - H + \frac{A^m}{H^s} \quad x \in (-1,1),\ t>0, \\ &A_x(\pm 1,t) = H_x(\pm 1,t) = 0,\ t>0, \end{aligned} \tag{1}$$

where all of the parameters are positive and (p,q,m,s) satisfy

$$1 < \frac{qm}{(s+1)(p-1)} < +\infty, \quad 1 < p < +\infty.$$

In all of the recent mathematical investigations it was assumed that the activator diffuses much slower than the inhibitor, that is

$$D_H \gg D_A, \tag{2}$$

1991 *Mathematics Subject Classification.* Primary 35B40, 35B45; Secondary 35J55, 92C15, 92C40.
Key words and phrases. Stability, Multiple-peaked solutions, Singular perturbations, Turing instability.

a condition which is related to those required for Turing instability [16]. See Chapter 2 of [10] for a thorough investigation. Mathematically, this assumption allows perturbation techniques to be employed, since the inhibitor can be assumed to be a slow-varying variable, and the system becomes only weakly coupled, as first observed in [15]. The activator then exhibits *spikes* – regions of steep gradients – separated by regions where the activator is nearly zero. For any given number N, a steady state containing N such spikes can be constructed. In [7] and [20] it was shown that there exists a sequence of numbers $D_1 > D_2 > \cdots$ (which has been given explicitly) such that if $D_H < D_N$ the symmetric N-spike solution is stable, while for $D_H > D_N$ the symmetric N-spike solution is unstable.

We now introduce the setting of this paper. In contrast with the above-mentioned works, we do not assume the large diffusivity ratio (2). Instead, we study the the limit of **large reaction rates of the activator**. More precisely, we assume that

$$p, m \gg 1 \quad \text{with } O\left(\frac{p}{m}\right) = 1. \tag{3}$$

To simplify our analysis, we make the following assumptions:

$$q = 1, \ s = 0. \tag{4}$$

Further, we require that

$$\tau = 0. \tag{5}$$

Assumption (5) will be important for the stability analysis. (We expect that the analysis in this paper can be extended to the case τ small enough with minor changes. When τ is sufficiently large, Hopf bifurcations can occur, see for example [19]. The analysis of the case τ large is more complicated, and is left for future work.) For convenience, we rewrite $m = (p-1)r$, $r = O(1)$. By rescaling the space as $x \to \sqrt{D_A}x$ and introducing $D = \frac{D_H}{D_A}$, $L = D_A^{-1/2}$, the system becomes

$$\begin{aligned} &A_t = A_{xx} - A + \frac{A^p}{H}; \quad \tau H_t = DH_{xx} - H + A^{(p-1)r}, \quad x \in (-L, L), \\ &A_x(\pm L) = 0 = H_x(\pm L), \\ &L, D = O(1); \quad p \gg 1; \quad r > 1 \text{ and } r = O(1). \end{aligned} \tag{6}$$

Now we describe some previous work and motivate the study of large reaction rates from biological applications.

Hunding and Engelhardt [5] considered the effect of large reaction rates on Turing's instability for several well-known reaction-diffusion systems (the Sel'kov model, Brusselator, Schnakenberg model, Gierer-Meinhardt system, Lengyel-Epstein model). By increasing the reaction rate (or the so-called Hill constant for Hill-type kinetics) which models cooperativity in the system, they showed, through a linearized stability

analysis, that pattern formation by Turing's mechanism is facilitated by large reaction rates, even when the ratio of the diffusion constants is close to one.

The Hill equation assumes that many molecules can interact simultaneously, which is not a very realistic assumption [21]. Instead, it is a more realistic physical assumption that one ligand molecule after another is being bound to a receptor. This can happen in basically two different ways: By a sequential binding mechanism, for which the order in which the sites are filled is determined, or an independent binding mechanism, for which the sites can be occupied independently. Although for these two processes the Hill number is smaller than the number of sites, they can still lead to high Hill numbers.

A interesting case study about the molecular basis of cooperative interactions has recently been given in [17]. The mechanism of the binding of Calcium ions to Calmodulin, a multi-site and multi-functional protein, has been modeled quantitatively and the theoretical results have been confirmed by experimental observations.

In [1] evidence has been found for the fact that protein subunits can degrade less rapidly when associated in multimeric complexes, an effect which is called cooperative stability.

The assumption of large reaction rates is reasonable for models of pattern formation induced by gene hierarchy due to their high degree of cooperativity [5]. High cooperativity plays an important role even for rather primitive animals and plants like flatworm, ciliates, fungi and has been well investigated in *Drosophila*. In the latter example the homeobox genes are known to play a major role [13], [22] in facilitating a high degree of cooperativity. Key ingredients of the gene hierarchy have been identified such as the maternal gene *bicoid*, the gap gene *hunchback* and the primary pair-rule genes, which are expressed in a series of seven equally spaced and precisely phase shifted stripes. The occurrence of these stripes can be explained by a Turing mechanism in combination with maternal and gap gene interactions. These mechanisms have been reviewed in [6], [11], and [12].

The reason why cooperativity for homeobox genes is high is their ability to create proteins which can bind to several other genes, in this process activating or inhibiting them. Experimentally reaction rates exceeding 8 have been found for several different gene control systems. (Note that even for $p = 8$ the steady state solution u constructed below is already very well approximates by a spike on a real line since its spatial decay rate is of the order $e^{-14|x|}$.) An explicit example is the pair rule gene *hairy* which was originally connected to the nervous system but plays a role in the initial body plan of *Drosophila* as well.

A high degree of cooperativity leads to a whole class of control systems with large reaction rates which can explain the emergence of a variety of complex patterns. These systems can read out and remember gradients in the positional information, a fact which is important since this information must often be used repeatedly for example in the anterior-posterior or dorsal-ventral gradients in *Drosophila*. The systems further have the

ability to react in an almost on-off manner to very shallow gradients in positional information, a property which plays a major role for example in controlling the cell cycle governing mitosis, where the properties of the system must change qualitatively if its size is increased by a factor two. Further behaviors of solutions to the resulting nonlinear systems include time oscillations and multi-stability, the latter being important for modeling cell differentiation.

In this paper, we give a first analysis on Turing's nonlinear patterns in the case of **large reaction rates**. The model we consider is the Gierer-Meinhardt system, although our analysis can be extended to other reaction-diffusion systems with large reaction rates (as in [5]).

We now present the main results of the paper. The first result is about the existence of steady states with one or two spikes which is formulated using the Sobolev space with Neumann boundary conditions defined by

$$H_N^2(-L,L) = \left\{ u \in H^2(-L,L) \,:\, u_z(-L) = u_z(L) = 0 \right\}.$$

Theorem 1. *(a) Consider the system*

$$0 = A_{xx} - A + \frac{A^p}{H}; \qquad 0 = DH_{xx} - H + A^{(p-1)r}, \tag{7}$$

where

$$x \in (-L,L), \qquad A_x(\pm L) = 0 = H_x(\pm L). \tag{8}$$

We assume that D, r, L are positive and fixed and set

$$\alpha := \frac{1}{p-1}.$$

If p is large enough (i.e. if α is small enough), then (7) admits a solution $(A,H) \in (H_N^2(-L,L))^2$ such that

$$A(x) = \begin{cases} \left(\frac{H_0\eta}{3\alpha}\right)^\alpha w^\alpha\left(\frac{\sqrt{\eta}}{\alpha}x\right)(1+O(\alpha)), & |x| \ll 1, \\ \frac{1}{\alpha^\alpha}\dfrac{\cosh(|x|-L)}{\cosh(L)}(1+O(\alpha)), & |x| \gg O(\alpha), \end{cases} \tag{9}$$

$$H(x) = H_0\frac{\cosh\left(\frac{|x|-L}{\sqrt{D}}\right)}{\cosh\left(\frac{L}{\sqrt{D}}\right)}(1+O(\alpha)), \tag{10}$$

where

$$\begin{aligned} H_0 &= \alpha\eta^{-\frac{r-1/2}{r-1}}\left[2\beta^{-1}D^{1/2}\tanh\left(\frac{L}{\sqrt{D}}\right)\right]^{1/(r-1)}(1+O(\alpha)), \\ \eta &= \tanh^2(L), \\ \beta &= \int_{-\infty}^{\infty}\left(\frac{1}{2}\right)^r \operatorname{sech}^{2r}\left(\frac{y}{2}\right)dy, \end{aligned}$$

and $w(y) = \frac{3}{2}\operatorname{sech}^2\left(\frac{y}{2}\right)$ is the unique ground state solution to

$$w_{yy} - w + w^2 = 0, \quad w > 0, \quad w_y(0) = 0, \quad w(y) \sim Ce^{-|y|}, \quad |y| \to \infty. \tag{11}$$

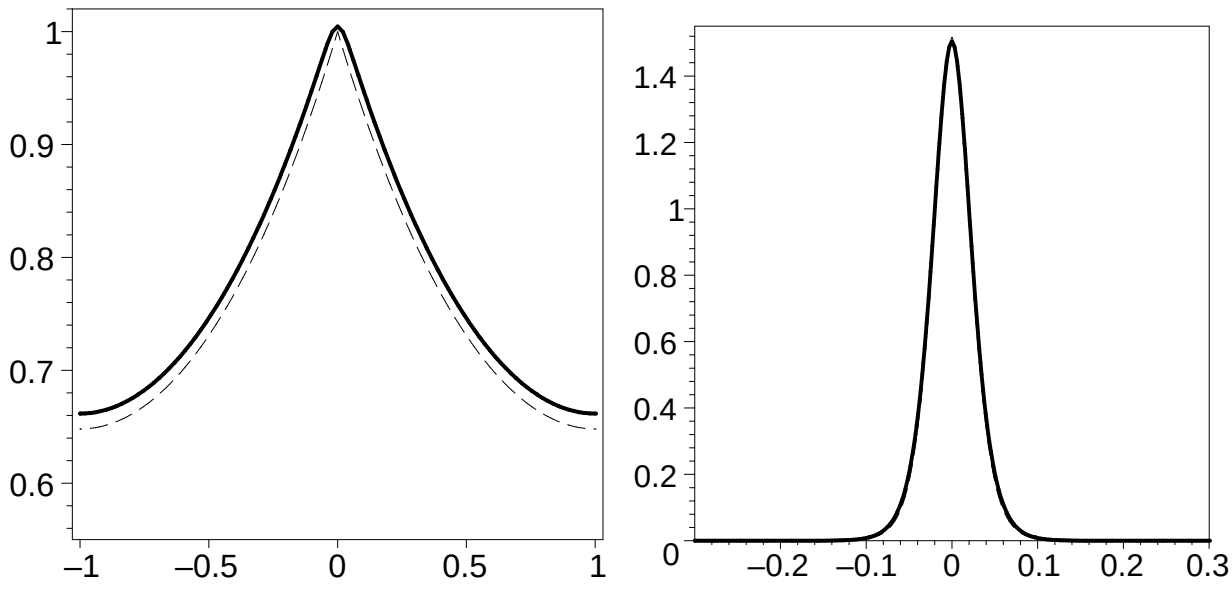

(a) (b)

FIGURE 1. (a) The plot of the steady state $A(x)$ (solid line) and its outer region asymptotic approximation (dashed line) given by $\cosh(|x|-L)/\cosh(L)$ (b) The plot of $A(x)^p$ near the origin. Its asymptotic approximation given by (9) is also drawn, but is indistiguishable by eye from the numerical solution. The parameter values are $p = 90$, $r = 2$, $D = 1$, $L = 1$. Note that A^p is localized near the origin, while A is not.

Further, the error is estimated in the following space:

$$\left\| \alpha A^{1/\alpha}(\alpha z) - \frac{H_0 \eta}{3} w\left(\sqrt{\eta} z\right) \right\|_{H^2(-L/\alpha, L/\alpha)} = O(\alpha).$$

(b) The restriction of the solution constructed in Part (a) to the interval $(0, L)$ is a solution $(A, H) \in (H_N^2(0, L))^2$ the system (7), where

$$A_x(0) = A_x(L) = 0 = H_x(0) = H_x(L). \tag{12}$$

(c) The extension of the solution constructed in Part (b) from the interval $(0, L)$ to interval $(0, 2L)$ by even reflection at $x = L$ is a solution $(A, H) \in (H_N^2(0, 2L))^2$ to the system (7), where

$$A_x(0) = A_x(2L) = 0 = H_x(0) = H_x(2L). \tag{13}$$

Remarks. *1. The steady state in (a) has an* interior spike *for A^p located in the center $x = 0$ of the interval. The solution in (b) has a* boundary spike *for A^p located at the left boundary $x = 0$. The solution in (c) has* two boundary spikes *for A^p located at the boundaries $x = 0$ and $x = 2L$.*

2. The key observation is that, unlike in the case of a slowly diffusing activator ($D_A \ll D_H$), the activator A does not look like a spike; nonetheless, its power A^p does. This is illustrated in Figure 1, where both A and A^p are plotted. Note that A^p is localized near the origin, while A is not.

3. A remarkable fact is that in the above theorem the ratio of the two diffusivities D can be any finite number.

4. We will construct these steady-state solutions in §2. The solutions each consist of an inner and outer region, and its construction is done by the method of matched asymptotics.

The second main result of this paper is the stability analysis for these solutions. We summarize it as follows.

Theorem 2. *Suppose p is large enough. Then we have the following results for the stability of the steady states constructed in Theorem 1:*

(a) The interior spike is unstable. The eigenvalue problem has an eigenvalue with positive real part of exact order $O(1)$ which is given in (67). The corresponding eigenfunction is an odd function.

(b) The boundary spike is stable.

(c) The steady state with two boundary spikes is stable if $D < D_c$ and it is unstable if $D > D_c$, where D_c is given by

$$D_c = \left(\frac{L}{\arctan\left(1/\sqrt{r}\right)} \right)^2. \tag{14}$$

If $D > D_c$ there is an eigenvalue λ with $Re(\lambda) = O(p^2)$. The corresponding eigenfunction is odd about $x = L$.

The two instabilities of Theorem 2 are shown in Figure 2. The instability of the interior spike induces spike motion towards the boundary and, due to the small eigenvalue, happens on a slow timescale $O(1)$. On the other hand, the instability of the boundary spike occurs on a much faster timescale $O(\frac{1}{p^2})$, corresponding to a "large" eigenvalue. As a result, one of the two boundary spikes is annihilated.

Note that a multi interior spike solution can be constructed from an interior spike solution by even reflection. However, since a single interior spike is unstable, this multi-spike configuration is also automatically unstable. This is because an eigenfunction corresponding to one interior spike can be extended by even reflection to an eigenfunction for K interior spikes. So an unstable mode of a single spike automatically induces an instability for K spikes.

Finally, it should be mentioned that both Theorem 1 and Theorem 2 can be made rigorous by the method of Liapunov-Schmidt reduction as used in [20]. We will give an outline of the proof of Theorem 1 in Remark 4 following the result.

We now summarize the contents of the paper. In §2 we use asymptotic analysis to construct the steady-state solution given in Theorem 1. In §3 we derive the eigenvalue problem. In §4 we consider the large eigenvalues and reduce the eigenvalue problem to a nonlocal eigenvalue problem. In Theorem 3 we fully classify its unstable eigenfunctions and their eigenvalues. When $r = 2$ we are able to obtain necessary and

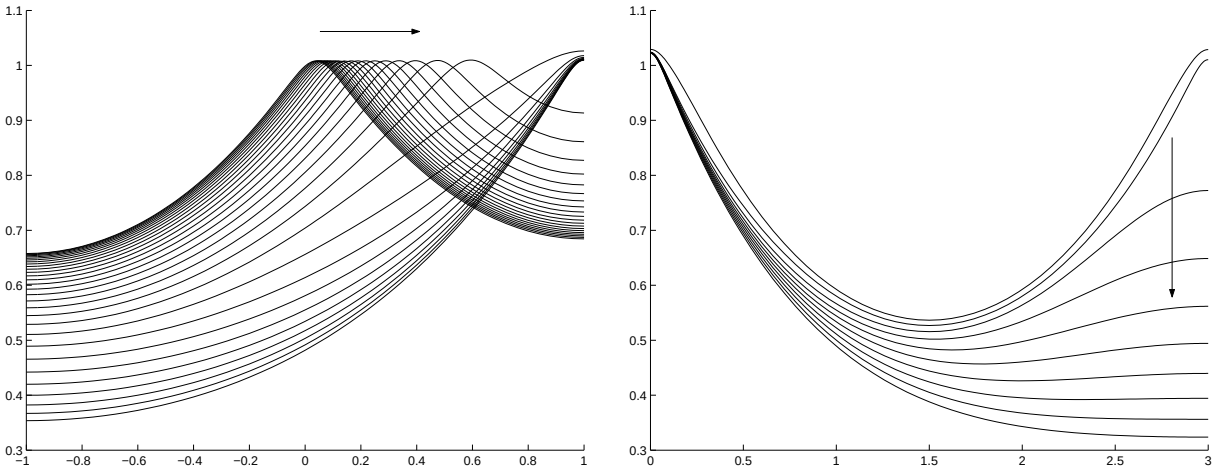

(a) (b)

FIGURE 2. (a) Motion of the interior spike towards the right boundary. Profiles of $A(x)$ are shown with increments of 0.1 time steps. The parameter values used were $p = 50$, $r = 2$, $D = 1$, $L = 1$. The initial condition was taken to be slightly to the right of the center. (b) Competition instability of two boundary spikes. The profiles of $A(x)$ are shown with increments of 0.1 time steps. The spike at the right boundary eventually disappears. Here, $p = 50$, $r = 2$, $D = 4$, $L = 1.5$ with $x \in (0, 2L)$.

sufficient conditions for stability. In Theorem 4 we state the corresponding result on a large bounded interval. In §5 we study the small eigenvalues. We show that all corresponding unstable eigenfunctions are odd. In §6 we apply the results of §4 and §5 to prove Theorem 2. Applying the results of §4, the stability of a boundary spike is established. Applying the results of §5 to the case of an interior spike, we show that there is a small eigenvalue with positive real part, so that an interior spike is unstable. Applying the results of §4 to the case of a double boundary spike, we show that there is a large eigenvalue whose real part is positive or negative, depending on the condition on $D < D_c$ or $D > D_c$ for some $D_c > 0$, respectively. All the other eigenvalues have negative real part, so the double boundary spike can be stable or unstable. In §7 we discuss our results, emphasize their relevance for pattern formation in reaction-diffusion systems and biological application, and we conclude by stating some open problems.

2. Construction of the steady state

In this section we construct the steady state usinig asymptotic matching and prove Theorem 1. As a motivation, note that a solution to the ODE

$$v_{xx} - v + v^p = 0, \quad x \in \mathbb{R},$$

is explicitly given by

$$v(x) = \left[\left(\frac{p+1}{2}\right)\operatorname{sech}^2\left(\frac{p-1}{2}x\right)\right]^{\frac{1}{p-1}}.$$

Taking into consideration the scalings of the spatial variable and of the amplitude of this solution, for $p \ll 1$, this motivates the following change of variables:

$$A(x) = \left(\frac{u(z)}{\alpha}\right)^{\alpha}, \quad z = \frac{x}{\alpha}, \tag{15}$$

where

$$\alpha = \frac{1}{p-1} \ll 1.$$

With this rescaling, we anticipate that u will be independent of p at the leading order. We then obtain the following *inner problem*:

$$\begin{aligned} 0 &= u_{zz} - \frac{u_z^2}{u} + \frac{u^2}{H} + \alpha\left(-u + \frac{u_z^2}{u}\right) + O(\alpha^2), \quad |z| \ll \frac{1}{\alpha}, \\ 0 &= \frac{1}{\alpha^2} D H_{zz} - H + u^r \alpha^{-r}. \end{aligned}$$

In the inner region $|z| \ll \frac{1}{\alpha}$ we expand

$$\begin{aligned} u(z) &= U_0(z)(1 + O(\alpha)), \\ H(z) &= H_0(1 + O(\alpha)). \end{aligned}$$

Below, we will show that $u = O(\alpha)$ and $H = O(\alpha)$ so that the leading order equations are

$$U_{0zz} - \frac{U_{0z}^2}{U_0} + \frac{U_0^2}{H_0} = 0, \quad H_{0,zz} = 0. \tag{16}$$

This, together with the boundary conditions, implies that H_0 is a constant. A direct verification shows that (16) admits a one-parameter family of solutions given by

$$U_0(z) = \frac{H_0}{3}\eta w\left(\sqrt{\eta} z\right),$$

where

$$w(y) = \frac{3}{2}\operatorname{sech}^2\left(\frac{y}{2}\right) \tag{17}$$

is a solution to (11) and where η is an arbitrary parameter that corresponds to a scaling symmetry $U_0 = \eta \hat{U}_0, \quad z = \eta^{-1/2}\hat{z}$ of (16). The values for η and H_0 are to be determined shortly.

In the inner region, we compute, using

$$w(y) = 6\exp(-|y|) + O(\exp(-2|y|)) \quad \text{as } |y| \to \infty,$$

that

$$\begin{aligned} A(z) &= \frac{1}{\alpha^\alpha}\exp\left(\alpha \ln u(z)\right) \\ &= \frac{1}{\alpha^\alpha}\exp\left(\alpha\ln(U_0(z)) + O(\alpha^2)\right) \\ &= \frac{1}{\alpha^\alpha}\left(1 - \alpha\sqrt{\eta}|z| + O(\alpha^2)\right) \quad \text{for } |z| \ll \frac{1}{\alpha}. \end{aligned} \tag{18}$$

It follows that $A(z) \to \frac{1}{\alpha^\alpha}$ as $|z| \to \infty$.

In the outer region $\alpha \ll |x|$ (equivalent to $1 \ll |z|$), we have

$$A_{xx} - A \sim 0; \quad A_x(\pm L) = 0$$

and the matching condition with the inner solution gives $A(0) = \frac{1}{\alpha^\alpha}$. This implies

$$A(x) = \frac{1}{\alpha^\alpha}\left(\frac{\cosh\left(L - |x|\right)}{\cosh L} + O(|x|^2)\right), \quad \alpha \ll |x|.$$

Next we perform the matching of the inner and outer solution to the next order. For $\alpha \ll |x| \ll 1$ we expand the outer solution in a Taylor series to get

$$\begin{aligned} A &= \frac{1}{\alpha^\alpha}\left(1 - (\tanh L)\,|x| + O(|x|^2)\right) \\ &= \frac{1}{\alpha^\alpha}\left(1 - \alpha\,(\tanh L)\,|z| + O\left(\alpha^2|z|^2\right)\right). \end{aligned} \tag{19}$$

Equating the $O(\alpha)$ terms in (18) and (19), we get

$$\eta = \tanh^2 L.$$

To compute H_0, we note that in the outer region, $|A^{(p-1)r}| = o(1)$. We therefore write

$$DH_{xx} - H \sim -C_0\delta\left(x\right); \quad H_x\left(\pm L\right) = 0,$$

where

$$\begin{aligned} C_0 &= \int_{-\infty}^{\infty} A^{(p-1)r}dx \\ &= \frac{\alpha}{\sqrt{\eta}}\left(\frac{H_0\eta}{3\alpha}\right)^r\int_{-\infty}^{\infty} w^r\,dy \\ &= \frac{\alpha}{\sqrt{\eta}}\left(\frac{H_0\eta}{\alpha}\right)^r\beta \end{aligned} \tag{20}$$

and

$$\beta = \int_{-\infty}^{\infty}\left(\frac{1}{2}\right)^r \operatorname{sech}^{2r}\left(\frac{y}{2}\right)\,dy.$$

It follows that

$$H(x) = B\cosh\left(\frac{L - |x|}{\sqrt{D}}\right)(1 + O(\alpha)),$$

where B is determined by

$$\sqrt{D}B\sinh\left(\frac{L}{\sqrt{D}}\right)=\frac{1}{2}C_0.$$

This implies that

$$H(0)=H_0\left(1+O(\alpha)\right)=\frac{1}{2}\frac{C_0}{\sqrt{D}}\coth\left(\frac{L}{\sqrt{D}}\right)\left(1+O(\alpha)\right),$$

$$H_0=\alpha\eta^{-\frac{r-1/2}{r-1}}\left[2\beta^{-1}D^{1/2}\tanh\left(\frac{L}{\sqrt{D}}\right)\right]^{1/(r-1)}\left(1+O(\alpha)\right). \tag{21}$$

Note that this verifies the consistency assumptions that $U_0=O\left(\alpha\right)$ and $H_0=O\left(\alpha\right)$, which were required in (16). This completes the construction of a boundary spike. The other two types of steady states (interior spike on $(-L,L)$, two boundary spikes on $(0,2L)$) follow from the boundary spike on $(0,L)$ by reflection at $x=0$ and $x=L$, respectively. This concludes the derivation of Theorem 1. ■

A rigorous proof of this result using Liapunov-Schmidt reduction and following the approach of [20] can be outlined as follows:

Note that for given $u\in H_N^2(-L/\alpha,L/\alpha)$, the solution $(A,H)\in(H_N^2(-L,L))^2$ can be expressed by using Green's function. Choosing a suitable approximation

$$u=\frac{H_0\eta}{3\alpha}w\left(\frac{\sqrt{\eta}}{\alpha}x\right)\left(1+O(\alpha)\right)$$

which satisfies the boundary condition $u_z(-L/\alpha)=u_z(L/\alpha)=0$, e.g. by using a cutoff function, it is not too hard too show that this approximation solves the Gierer-Meinhardt system (7) up to an error of the order $O(\alpha)$ in the norm of the space $(L^2(-L/\alpha,L/\alpha))^2$. Then, using Liapunov-Schmidt reduction, the proof can be completed and an exact solution can be determined. The value of the constant η is calculated as part of the process.

3. Stability

We now study the linear stability of the non-homogeneous steady state. Linearize around the steady state as:

$$A(x,t)=A(x)+e^{\lambda t}\phi(x),$$

$$H(x,t)=H(x)+e^{\lambda t}\psi(x),$$

where $(A(x),H(x))$ is the steady state solution as given by Theorem 1. We obtain

$$\lambda\phi=\phi_{xx}-\phi+p\frac{A^{p-1}\phi}{H}-\frac{A^p}{H^2}\psi, \tag{22a}$$

$$0=D\psi_{xx}-\psi+r\left(p-1\right)A^{(p-1)r-1}\phi. \tag{22b}$$

As before, we make the change of variables given in (15). Since $A\sim 1$ near $x\sim 0$ we have

$$A^p=\frac{u}{\alpha}A\sim\frac{u}{\alpha}.$$

We obtain

$$\alpha^2(\lambda+1)\phi \sim \alpha^2\phi_{xx} + \frac{u}{H}\phi + \alpha\frac{u}{H}\phi - \alpha\frac{u}{H^2}\psi, \tag{23}$$

$$0 \sim D\psi_{xx} - \psi + r\alpha^{-r-1}u^r\phi. \tag{24}$$

For an interior spike which is symmetric about the origin, there are two possible types of eigenfunctions: either odd or even around the origin. Both satisfy Neumann boundary conditions on $(-L, L)$. This yields two separate problems. An even eigenfunction can be restricted to $(0, L)$ and is the same as an eigenfunction for a single boundary spike.

Finally, the double boundary spike on $(0, 2L)$ requires an extra type of eigenfunction which is odd about $x = L$. This leads to three different types of eigenfunctions which $(0, L)$, whose boundary conditions and symmetry properties are specified as follows:

- **Even eigenfunction for an interior spike on** $(-L, L)$ **or a boundary spike on** $(0, L)$:

$$\phi_x(0) = 0,\ \phi_x(L) = 0;\ \psi_x(0) = 0,\ \psi_x(L) = 0; \tag{25}$$

- **Odd eigenfunction for an interior spike on** $(-L, L)$**:**

$$\phi(0) = 0,\ \phi_x(L) = 0;\quad \psi(0) = 0,\ \psi_x(L) = 0; \tag{26}$$

- **Eigenfunction which is odd about** $x = L$ **for a double boundary spike on** $(0, 2L)$**:**

$$\phi_x(0) = 0,\ \phi(L) = 0;\ \psi_x(0) = 0,\ \psi(L) = 0. \tag{27}$$

As will be evident shortly, problems (25) and (27) admit eigenvalues that have $O(p^2)$. We will refer to these as *large eigenvalues*. These are analyzed in §4. On the other hand, problem (26) admits an eigenvalue of $O(1)$ which is studied in §5. We will refer to it as the *small eigenvalue*.

4. Large eigenvalues

We start by analyzing the large eigenvalues. Changing to inner variables, we have

$$x = \frac{\alpha}{\sqrt{\eta}}y; \quad u \sim \frac{H_0}{3}\eta w(y);$$

and we obtain

$$\frac{\alpha^2}{\eta}(\lambda+1)\phi \sim \phi_{yy} + \frac{1}{3}w\phi - \frac{\alpha}{3}\frac{\psi_0}{H_0}w,$$

where

$$\psi_0 = \psi(0)$$

and $\psi(0)$ is determined by

$$D\psi_{xx} - \psi \sim C_1\delta(x);\quad \psi_x(\pm L) = 0, \tag{28}$$

$$C_1 = \int_{-\infty}^{\infty} \left(\frac{u}{\alpha}\right)^r \frac{r}{\alpha}\phi\, dx = \frac{r}{\sqrt{\eta}} \left(\frac{H_0\eta}{3\alpha}\right)^r \int_{-\infty}^{\infty} w^r \phi\, dy.$$

This implies that

$$\psi(x) = -C_1 G(0),$$

where

$$G(x) = \frac{\cosh\left(\frac{L-|x|}{\sqrt{D}}\right)}{2\sqrt{D}\sinh\left(\frac{L}{\sqrt{D}}\right)}$$

is the Green's function satisfying

$$DG_{xx} - G = -\delta(x), \quad G_x(\pm L) = 0.$$

On the other hand, from (21) we have

$$H_0 = \frac{\alpha}{\sqrt{\eta}} \left(\frac{H_0\eta}{3\alpha}\right)^r \int_{-\infty}^{\infty} w^r\, dy\, G(0).$$

So the boundary conditions (25) lead to following dimensionless nonlocal eigenvalue problem:

$$\lambda_0\phi = \phi_{yy} + \frac{1}{3}w\phi - \frac{r}{3}w\frac{\int_{-\infty}^{\infty} w^r\phi\, dy}{\int_{-\infty}^{\infty} w^r\, dy}, \qquad \lambda_0 \sim \frac{\alpha^2}{\eta}\lambda. \tag{29}$$

For the boundary conditions (27), the only difference is that the boundary conditions in (28) are changed to Dirichlet conditions $\psi(\pm L) = 0$. Thus the Green's function now is the one for Dirichlet boundary conditions given by

$$G_d(x) = \frac{\sinh\left(\frac{L-|x|}{\sqrt{D}}\right)}{2\sqrt{D}\cosh\left(\frac{L}{\sqrt{D}}\right)}.$$

A similar computation then leads to:

$$\lambda_0\phi = \phi_{yy} + \frac{1}{3}w\phi - \frac{r}{3}\tanh^2\left(\frac{L}{\sqrt{D}}\right) w\frac{\int_{-\infty}^{\infty} w^r\phi\, dy}{\int_{-\infty}^{\infty} w^r\, dy}, \qquad \lambda_0 \sim \frac{\alpha^2}{\eta}\lambda. \tag{30}$$

Equations (29), (30) are the starting point of our analysis. Both cases will be covered, once we prove the following two key theorems.

Theorem 3. *Let*

$$L_0\phi = \phi_{yy} + \frac{1}{3}w\phi \tag{31}$$

and consider the following nonlocal eigenvalue problem on all of $\mathbb{R}$ *:*

$$L_0\phi - \gamma w\int_{-\infty}^{\infty} w^r\phi\, dy = \lambda\phi, \quad \phi \in L^\infty(\mathbb{R}),\ r \geq 1 \tag{32}$$

where w *is given by (11). Let*

$$\gamma_0 = \frac{1}{3}\frac{1}{\int_{-\infty}^{\infty} w^r\, dy}. \tag{33}$$

We have the following:

(a) If $\gamma < \gamma_0$ *then (32) has a positive eigenvalue* $\lambda > 0$.

(b) If $\gamma > \gamma_0$ and $r = 2$ then $\mathrm{Re}(\lambda) \le 0$ for all λ. The only eigenfunction corresponding to $\lambda = 0$ is $\phi = \frac{w_y}{w}$ which is an odd function; all other eigenvalues have strictly negative real part.

Remark: *We conjecture that (b) is true for all $r \ge 1$. In fact one can show that (b) is true also when $r = 1$ (in this case the eigenvalues are purely real because the operator in (32) is self-adjoint). We do not know how to prove (b) for general r. However, we see no reason why the result should not be true for general r, for example there do not seem to be any bifurcations in the system for changing r.*

Strictly speaking, the inner problem (32) is actually posed on a finite but large interval $(-R, R)$ with $R = L/\alpha$. However, this does not affect the stability of the large eigenvalues, as we demonstrate in the following theorem.

Theorem 4. *Let $R > 0$ and consider the nonlocal eigenvalue problem on $(-R, R)$:*

$$L_0\phi - \gamma w \int_{-R}^{R} w^r \phi \, dy = \lambda_R \phi, \ \phi \in L^\infty(-R, R), \ \phi_y(\pm R) = 0, \ r \ge 1. \tag{34}$$

Then there exists $R_0 > 0$ such that for $R > R_0$, we have the following:

(a) If $\gamma < \gamma_0$, then (34) has a positive eigenvalue $\lambda_R > 0$.

(b) If $\gamma > \gamma_0$ and $r = 2$, then either $\lim_{R\to\infty} \lambda_R = 0$ or $\mathrm{Re}(\lambda_R) \le -c_0$ for some $c_0 > 0$.

Note that Theorems 3 and 4 imply the threshold (14). It also shows that the interior spike is stable with respect to even perturbations.

Before proving Theorem 3, we first summarize the properties of the local operator L_0. Note that

$$L_0 w = w - \frac{2}{3} w^2; \quad L_0^{-1} w = 3 \tag{35}$$

$$\int_{-\infty}^{\infty} w^2 \, dy = 6; \quad \int_{-\infty}^{\infty} w \, dy = 6. \tag{36}$$

In addition we have the following characterization of the spectrum of L_0.

Lemma 5. *The eigenvalue problem*

$$L_0\phi = \phi_{yy} + \frac{1}{3} w\phi = \lambda\phi, \quad \phi \in L^\infty(\mathbb{R}) \tag{37}$$

has two nonnegative eigenvalues. The first eigenvalue is

$$\lambda_1 = \frac{1}{4}$$

corresponding to an even eigenfunction given by

$$\phi_1 = w^{1/2}.$$

The second eigenvalue is

$$\lambda_2 = 0$$

corresponding to an odd eigenfunction given by

$$\phi_2 = \frac{w_y}{w}.$$

All other eigenvalues satisfy $\lambda < 0$ and are embedded in the continuous spectrum covering the negative real axis.

Finally, we will need the following key lemma.

Lemma 6. *Consider the eigenvalue problem*

$$L_0\phi - \frac{1}{18}w\int_{-\infty}^{\infty} w\phi\, dy = \lambda\phi,\ \ \phi \in L^\infty(\mathbb{R}). \tag{38}$$

It admits an eigenvalue $\lambda = 0$ whose eigenspace is spanned by the even eigenfunction $\phi = 1$ and the odd eigenfunction $\phi = \frac{w_y}{w}$. All other eigenvalues satisfy $\lambda < 0$. As a consequence, we have the following inequality

$$\int_{-\infty}^{\infty}\left((\phi_y)^2 - \frac{1}{3}w\phi^2\right)dy + \frac{1}{18}\left(\int_{-\infty}^{\infty} w\phi\, dy\right)^2 \geq 0, \quad \forall\ \phi \in H^1(\mathbb{R}). \tag{39}$$

Proof of Lemma 5. We proceed as in [2]. Let $\gamma = \sqrt{\lambda}$, where we take the principal branch of the square root. Next, substitute $\phi(y) = w^\gamma(y)F(y)$. Then F satisfies

$$F_{yy} + 2\gamma\frac{w_y}{w}F_y + \left(\frac{1}{3} - \left(\gamma + \frac{2}{3}\gamma(\gamma-1)\right)\right)wF = 0. \tag{40}$$

We introduce the following new variable

$$z = \frac{1}{2}\left(1 - \frac{w_y}{w}\right). \tag{41}$$

Then

$$\frac{w_y}{w} = 1 - 2z, \quad w = 6z(1-z), \quad \frac{dz}{dx} = z(1-z).$$

This gives the following equation for F as a function of z:

$$z(1-z)F^{''} + (c - (a+b+1)z)F^{'} - abF = 0, \tag{42}$$

where

$$a + b + 1 = 2 + 4\gamma, \quad ab = 2(2\gamma(\gamma-1) - 3(\frac{1}{3} - \gamma)), \quad c = 1 + 2\gamma. \tag{43}$$

The solutions to (42) are standard hypergeometric functions. See [14] for more details. Now there are two solutions to (42):

$$F(a,b;c;z) \quad \text{and} \quad z^{1-c}F(a-c+1, b-c+1; 2-c; z).$$

By our construction, F is regular at $z = 0$. At $z = 1$, $F(a,b;c;z)$ has a singularity

$$\lim_{z\to 1}(1-z)^{-(c-a-b)}F(a,b;c;z) = \frac{\Gamma(c)\Gamma(a+b-c)}{\Gamma(a)\Gamma(b)},$$

where $c-a-b=-2\gamma<0$. Note that since $\gamma=\sqrt{\lambda}$, the real part of γ is positive. So a solution that is regular at both $z=0$ and $z=1$ can only exist if $\Gamma(x)$ has a pole at a or b, respectively. In other words, we have

$$a=0,-1,-2,\dots \text{ or } b=0,-1,-2,\dots. \tag{44}$$

From (43), we compute that

$$a=2\gamma-1,\quad b=2\gamma+2 \qquad \text{or} \qquad b=2\gamma-1,\quad a=2\gamma+2.$$

By assumption, $\mathrm{Re}(\gamma)\geq 0$, so we must choose either $\gamma=0$ or $\gamma=\frac{1}{2}$ in order to satisfy (44).This gives

$$\lambda=\frac{1}{4} \text{ or } \lambda=0.$$

In case $\lambda=\frac{1}{4}$, we have $\gamma=1/2,\ a=0,\ b=3,\ \ c=2,\ \ F(0,3;2;z)=1$. Thus the corresponding eigenfunction is $w^{1/2}$ (taking $a=3,b=0$ also yields the same eigenfunction). In case $\lambda=0$ we get $a=-1,b=2,c=1$. Now $F(-1,2,1,z)=1-2z$ and it then follows from (41) that $\phi=\frac{w_y}{w}$. This concludes the proof of the first part of the lemma. Standard spectral properties of elliptic operators in combination with these results imply the second part of the lemma. ■

Proof of Lemma 6. We consider two cases. First, if

$$\int_{-\infty}^{\infty} w\phi\,dy=0, \tag{45}$$

then we have $L_0\phi=\lambda\phi$. Then by Lemma 5 either $\phi=Cw^{1/2}$, $\lambda=\frac{1}{4}$ or $\phi=C\frac{w_y}{w}$, $\lambda=0$, where C is some nonzero constant. The former case contradicts (45) since $w>0$; so only the latter case is possible. Moreover, since w is even, any odd eigenfunction ϕ satisfies (45) and hence by Lemma 5 must be equal to a multiple of $\phi=\frac{w_y}{w}$, corresponding to zero eigenvalue.

Next suppose that (45) does not hold. Since ϕ is defined up to a constant multiple, we may rescale it so that

$$\int_{-\infty}^{\infty} w\phi\,dy=18;$$

equation (38) then becomes

$$(L_0-\lambda)\phi=w.$$

Defining

$$f(\lambda)\equiv\int_{-\infty}^{\infty} w(L_0-\lambda)^{-1}w\,dy,$$

then λ solves the equation

$$f(\lambda)=18. \tag{46}$$

Since (38) is self-adjoint, all its eigenvalues are real and it suffices to show that $f(\lambda) \neq 18$ for $\lambda > 0$. Note that

$$L_0 1 = \frac{1}{3} w \tag{47}$$

so that

$$f(0) = 18 \tag{48}$$

and therefore $\lambda = 0$ is an eigenvalue of (38) corresponding to the eigenfunction $\phi = 1$. Next, we compute

$$f'(\lambda) = \int_{-\infty}^{\infty} w(L_0 - \lambda)^{-2} w \, dy = \int_{-\infty}^{\infty} \left[(L_0 - \lambda)^{-1} w\right]^2 \, dy > 0$$

so that $f(\lambda)$ is an increasing function. Finally, note that the local operator L_0 admits a single positive eigenvalue $\lambda_0 = \frac{1}{4}$. This implies that $f(\lambda)$ has a single pole at $\lambda = \frac{1}{4}$ and no other poles along the positive real axis $\lambda > 0$. On the other hand, for large values of λ we have

$$f(\lambda) \sim -\frac{1}{\lambda} \int_{-\infty}^{\infty} w^2 \, dy \to 0^- \text{ as } \lambda \to +\infty.$$

To summarize, $f(\lambda)$ has a vertical asymptote at $\lambda = \frac{1}{4}$; $f(0) = 18$, $f \to 0^-$ as $\lambda \to \infty$ and f is increasing for $\lambda \neq \frac{1}{4}$. It follows that $f(\lambda) \neq 18$ for all $\lambda > 0$ and this proves the lemma. To prove (39), we proceed by contradiction. Suppose (39) does not hold. Then we have a function $\phi \in H^1(\mathbb{R})$ such that

$$\int_{\mathbb{R}} \left(|\phi_y|^2 - \frac{1}{3} w \phi^2 \right) dy + \frac{1}{18} \left(\int_{\mathbb{R}} w \phi \, dy \right)^2 < 0 \tag{49}$$

which implies that for R large, the first eigenvalue for the following eigenvalue problem

$$L_0 \phi_R - \frac{1}{18} w \int_{-R}^{R} w \phi_R \, dy = \lambda_R \phi_R, \quad y \in (-R, R), \quad \phi_R(\pm R) = 0 \tag{50}$$

is positive. In fact,

$$-\lambda_R = \inf_{\int_{-R}^{R} \phi^2 \, dy = 1, \, \phi \in H_0^1(-R,R)} \int_{-R}^{R} \left((\phi_y)^2 - \frac{1}{3} w \phi^2 \right) dy + \frac{1}{18} \left(\int_{-R}^{R} w \phi \, dy \right)^2. \tag{51}$$

Thus $0 < \lambda_R$. Moreover, by (49), $\lambda_R \geq \lambda_0 > 0$ for R large. We may also assume that $\max_{y \in (-R,R)} \phi_R(y) = 1$. Letting $R \to +\infty$ and $\lambda_R \to \lambda$, we see that $\phi_R \to \phi$ which satisfies (38) with $\lambda > 0$. This is impossible. ■

Proof of Theorem 3. We start with the proof of (a).

Define a function

$$f(\lambda) \equiv \int_{-\infty}^{\infty} w^r (L_0 - \lambda)^{-1} w \, dy \tag{52}$$

so that the eigenvalue λ solves the equation

$$f(\lambda) = \frac{1}{\gamma}. \tag{53}$$

By (35), note that

$$f(0) = \frac{1}{\gamma_0} < \frac{1}{\gamma}. \tag{54}$$

Note that the local operator L_0 admits a single positive eigenvalue $\lambda_0 = \frac{1}{4}$. We claim that

$$f(\lambda) \to +\infty \text{ as } \lambda \to \lambda_0^-. \tag{55}$$

To see this, let $\lambda = \lambda_0 + \delta$ with $\delta \ll 1$ and let $\phi = (L_0 - \lambda)^{-1} w$. That is, ϕ satisfies

$$(L_0 - \lambda_0)\,\phi - \delta\phi = w.$$

Let $\phi_0 = w^{1/2}$ be the eigenfunction corresponding λ_0. We project w onto ϕ_0 so that we write

$$w = a\phi_0 + w_1; \qquad a = \frac{\int_{-\infty}^{\infty} w\phi_0\, dy}{\int_{-\infty}^{\infty} \phi_0^2\, dy}.$$

Therefore in the limit $\delta \to 0$, we get

$$\phi \sim -\frac{a}{\delta}\phi_0 + O(1), \qquad \delta \ll 1.$$

Hence we get

$$f(\lambda_0 + \delta) \sim -\frac{1}{\delta}\frac{\int_{-\infty}^{\infty} w\phi_0 \int_{-\infty}^{\infty} w^r\phi_0}{\int_{-\infty}^{\infty} \phi_0^2}, \quad \delta \to 0.$$

Since w and ϕ_0 are positive, this proves (55). On the other hand, $f(\lambda)$ has no other vertical asymptotes since L_0 has only one positive eigenvalue λ_0. It follows that (53) has a solution with $\lambda < 0 \le \lambda_0$ whenever $0 \le \gamma < \gamma_0$. This implies part (a).

Next we prove part (b). Since the operator (32) is not self-adjoint, the eigenvalues are in general complex. Therefore we write

$$\lambda = \lambda^r + \sqrt{-1}\lambda^i$$
$$\phi = \phi^r + \sqrt{-1}\phi^i.$$

When $r = 2$, we have

$$L_0\phi^r - \gamma w \int_{-\infty}^{\infty} w^2\phi^r\, dy = \lambda^r\phi^r - \lambda^i\phi^i \tag{56}$$

$$L_0\phi^i - \gamma w \int_{-\infty}^{\infty} w^2\phi^i\, dy = \lambda^r\phi^i + \lambda^i\phi^r. \tag{57}$$

Multiply (56) by ϕ^r and (57) by ϕ^i, then integrate and add to obtain

$$\int_{-\infty}^{\infty} \left(\phi^r L_0\phi^r + \phi^i L_0\phi^i\right)\, dy - \gamma A = \lambda^r B \tag{58}$$

where

$$A = \int_{-\infty}^{\infty} w\phi^r\, dy \int_{-\infty}^{\infty} w^2\phi^r\, dy + \int_{-\infty}^{\infty} w\phi^i\, dy \int_{-\infty}^{\infty} w^2\phi^i\, dy; \tag{59}$$

$$B = \int_{-\infty}^{\infty} ((\phi^r)^2 + (\phi^i)^2)\, dy. \tag{60}$$

Multiply (56) and (57) by w, integrate, then use integration by parts. This yields

$$\int_{-\infty}^{\infty} \phi^r \left(w - \frac{2}{3}w^2 \right) dy - 6\gamma \int_{-\infty}^{\infty} w^2 \phi^r \, dy = \lambda^r \int_{-\infty}^{\infty} \phi^r w \, dy - \lambda^i \int_{-\infty}^{\infty} \phi^i w \, dy$$
$$\int_{-\infty}^{\infty} \phi^i \left(w - \frac{2}{3}w^2 \right) dy - 6\gamma \int_{-\infty}^{\infty} w^2 \phi^i \, dy = \lambda^r \int_{-\infty}^{\infty} \phi^i w \, dy + \lambda^i \int_{-\infty}^{\infty} \phi^r w \, dy.$$

Eliminating λ^i we then obtain

$$(\lambda^r - 1)\, C + \left(\frac{2}{3} + 6\gamma \right) A = 0 \tag{61}$$

where A is given by (59) and

$$C = \left(\int_{-\infty}^{\infty} w\phi^r \, dy \right)^2 + \left(\int_{-\infty}^{\infty} w\phi^i \, dy \right)^2.$$

Next we use the following estimate, see Lemma 6:

$$\int_{-\infty}^{\infty} \phi L_0 \phi \, dy \le \frac{1}{18} \left(\int w\phi \, dy \right)^2.$$

Then (58) becomes

$$\lambda^r B + \gamma A \le \frac{1}{18} C.$$

Combining with (61) we obtain

$$\lambda^r B - \gamma \frac{(\lambda^r - 1)}{\left(\frac{2}{3} + 6\gamma \right)} C - \frac{1}{18} C \le 0$$

and so

$$\lambda^r \left[B - \frac{\gamma}{\left(\frac{2}{3} + 6\gamma \right)} C \right] \le \left[\frac{1}{18} - \frac{\gamma}{\left(\frac{2}{3} + 6\gamma \right)} \right] C. \tag{62}$$

Note that

$$\gamma_0 = \frac{1}{18}; \tag{63}$$

$$\frac{1}{18} \le \frac{\gamma}{\left(\frac{2}{3} + 6\gamma \right)} < \frac{1}{6} \quad \text{whenever } \gamma_0 \le \gamma < \infty \tag{64}$$

so that

$$\lambda^r \left[B - \frac{\gamma}{\left(\frac{2}{3} + 6\gamma \right)} C \right] \le 0, \quad \gamma \ge \gamma_0.$$

Now by Cauchy-Schwarz inequality we have

$$C \le 6B \iff B - \frac{1}{6} C \ge 0. \tag{65}$$

Combining (64) and (65) we have

$$B - \frac{\gamma}{\left(\frac{2}{3} + 6\gamma \right)} C \ge 0.$$

Therefore $\lambda^r \le 0$. Further, if $\lambda^r = 0$, then from (62) and (64) we have

$$0 \le \left[\frac{1}{18} - \frac{\gamma}{\left(\frac{2}{3} + 6\gamma \right)} \right] C \le 0;$$

this can only happen if $\gamma = \frac{1}{18} = \gamma_0$. This case is excluded from the assumption of Theorem 3. Therefore, $\lambda_r < 0$. ■

Proof of Theorem 4. Notice that since L_0 is self-adjoint, L_0 admits a single positive eigenvalue $\lambda_{0,R} = \frac{1}{4} + o(1)$ for R large. Part (a) follows from a simple perturbation argument.

To prove part (b), we proceed by contradiction. Suppose that for R large problem (34) has an eigenfunction ϕ with eigenvalue λ_R such that $\mathrm{Re}(\lambda_R) \geq -c_0$ for some $c_0 > 0$ independent of R small enough. We decompose ϕ into a sum of an odd and an even function. If ϕ is odd, then $\int_{-R}^{R} w^r \phi \, dy = 0$ and (34) is reduced to

$$L_0\phi = \lambda_R \phi, \quad \phi \in L^\infty(-R, R), \quad \phi \text{ is odd, } \phi_y(\pm R) = 0.$$

Thus by Lemma 5 we conclude that $\lambda_R \to 0$ as $R \to +\infty$ which implies the first alternative in Theorem 4 (b).

Suppose ϕ is even. Similar to the proof of Theorem 3, we have

$$\int_{-R}^{R} \left(\phi^r L_0 \phi^r + \phi^i L_0 \phi^i\right) dy - \gamma A = \lambda_R^r B \tag{66}$$

where λ_R^r is the real part of λ_R and $\phi = \phi^r + \sqrt{-1}\phi^i$. Thus $|\lambda_R^r| \leq C$ where C is independent of R for R large. Similarly, we also have that $|\lambda_R^i| \leq C$. Thus $|\lambda_R| \leq C$. Therefore we may assume that $\lambda_R \to \lambda$ as $R \to +\infty$. Since without loss of generality $||\phi||_{L^\infty(-R,R)} \leq 1$, the limit of ϕ exists and satisfies (32) with $\mathrm{Re}(\lambda) \geq -c_0$ for some $c_0 > 0$ and ϕ being even, which gives a contradiction to Theorem 3 (b) if c_0 is chosen small enough. Thus this is not possible and Theorem 4 (b) follows. ■

5. Small eigenvalue

It remains to study the stability of small eigenvalues. In particular, we prove the following result.

Theorem 7. *Consider the eigenvalue problem (22a,22b) with the boundary conditions (26). If $p \gg 1$ this problem admits a positive eigenvalue λ that satisfies*

$$\sqrt{\lambda+1}\tanh L \tanh\left(L\sqrt{\lambda+1}\right) = 1 + O\left(\frac{1}{p}\right). \tag{67}$$

To start with, expand the inner region to two orders for both the eigenfunction and the steady state:

$$x = \alpha z;$$

$$u = U_0(z) + \alpha U_1(z) + \cdots \qquad H = H_0 + \alpha H_1(z) + \cdots$$

$$\phi = \Phi_0(z) + \alpha \Phi_1(z) + \cdots \qquad \Psi = \Psi_0 + \cdots$$

The leading order equations are

$$\Phi_{0zz} + \frac{U_0}{H_0}\Phi_0 = 0; \qquad U_{0z} - \frac{U_{0z}^2}{U_0} + \frac{U_0^2}{H_0} = 0; \quad H_0 \equiv \text{const.} \tag{68}$$

The solution to Φ_0 is given by

$$\Phi_0(z) = \frac{U_{0z}}{U_0}. \tag{69}$$

We now formulate a solvability condition with Φ_0 as a test function. Multiplying (23) by $\frac{1}{\alpha}\Phi_0(\frac{x}{\alpha})$ and integrating on the half-interval $(0, L)$, we have,

$$\alpha^2(\lambda+1)\int_0^L \phi(x)\Phi_0(\frac{x}{\alpha})\frac{dx}{\alpha} = \int_0^L \left(\alpha^2\phi_{xx} + \frac{u}{H}\phi + \alpha\frac{u}{H}\phi - \alpha\frac{u}{H^2}\psi\right)(x)\Phi_0(\frac{x}{\alpha})\frac{dx}{\alpha}. \tag{70}$$

First we estimate the left hand side of (70). In the outer region we use $w(y) \sim C\exp(-|y|)$, $|y| \to \infty$ so that

$$\Phi_0 \sim -\sqrt{\eta}, \quad z \gg 1.$$

On the other hand, up to exponentially small terms we have

$$\phi_{xx} \sim (\lambda+1)\,\phi, \quad |x| \gg \alpha; \quad \phi_x\,(L) = 0$$

so that we may write

$$\phi \sim A_0 \frac{\cosh\left(\sqrt{\lambda+1}(x-L)\right)}{\cosh\left(\sqrt{\lambda+1}L\right)}$$

where A_0 is obtained by matching ϕ as $x \to 0$ to Φ_0 as $z \to \infty$. This yields

$$A_0 = -\sqrt{\eta}.$$

Therefore we estimate

$$\begin{aligned}\int_0^L \phi(x)\Phi_0(\frac{x}{\alpha})\,dx &\sim \eta\int_0^L \frac{\cosh\left(\sqrt{\lambda+1}(x-L)\right)}{\cosh\left(\sqrt{\lambda+1}L\right)}dx \\ &\sim \frac{\eta}{\sqrt{\lambda+1}}\tanh\left(\sqrt{\lambda+1}L\right)\end{aligned}$$

and finally

$$\text{lhs}(70) = \alpha\eta\sqrt{\lambda+1}\tanh\left(\sqrt{\lambda+1}L\right). \tag{71}$$

Next we must estimate the right hand side of (70). Since u decays exponentially as $z \to \infty$, the inner region provides the dominant contribution there. After changing variables $x = \alpha z$ and expanding, we obtain,

$$\begin{aligned}\text{rhs}(70) = &\int_0^\infty \Phi_0\left(\Phi_{0zz} + \frac{U_0}{H_0}\Phi_0\right)dz + \alpha\int_0^\infty \Phi_0\left(\Phi_{1zz} + \Phi_1\frac{U_0}{H_0}\right)dz \\ &+ \alpha\int_0^\infty \Phi_0^2\left(\frac{U_1}{H_0} - \frac{U_0H_1}{H_0^2}\right)dz + \alpha\int_0^\infty \frac{U_0\Phi_0^2}{H_0} - \alpha\int_0^\infty \frac{U_0\Phi_0}{H_0^1}\Psi_0\,dz + O(\alpha^2).\end{aligned}$$

The first term is zero by (68); we write the remaining terms as

$$\text{rhs}(70) = \alpha(I_0 + I_1 + I_2 + I_3)$$

where

$$\begin{aligned}I_0 &= \int_0^\infty \Phi_0\left(\Phi_{1zz} + \Phi_1\frac{U_0}{H_0}\right)dz \\ I_1 &= \int_0^\infty \Phi_0^2\left(\frac{U_1}{H_0} - \frac{U_0H_1}{H_0^2}\right)dz \\ I_2 &= \int \Phi_0^2\frac{U_0}{H_0}\,dz \\ I_3 &= -\int_0^\infty \frac{U_0\Phi_0}{H_0^2}\Psi_0\,dz.\end{aligned}$$

Now define

$$L_0\Phi \equiv \Phi_{zz} + \frac{U_0}{H_0}\Phi.$$

First, we integrate by parts to obtain

$$I_0 = \int_0^\infty \Phi_0 L_0 \Phi_1 \, dz = [\Phi_{1z}\Phi_0 - \Phi_1\Phi_{0z}]_0^\infty = 0.$$

Next, U_1 satisfies

$$U_{1zz} - \frac{2U_{0z}U_{1z}}{U_0} + \frac{U_{0z}^2}{U_0^2}U_1 + 2\frac{U_0U_1}{H_0} - \frac{U_0^2}{H_0^2}H_1 - U_0 + \frac{U_{0z}^2}{U_0} = 0. \tag{72}$$

Now define

$$\hat{U}_1 \equiv \frac{U_1}{U_0}.$$

Then $\hat{U}_1$ satisfies

$$\hat{U}_{1zz} + \frac{U_0}{H_0}\hat{U}_1 - \frac{U_0H_1}{H_0^2} - 1 + \frac{U_{0z}^2}{U_0^2} = 0. \tag{73}$$

Differentiating (73) we obtain

$$\begin{aligned} L_0\hat{U}_{1z} &= -\frac{U_{0z}\hat{U}_1}{H_0} + \frac{U_{0z}H_1}{H_0^2} + \frac{U_0H_{1z}}{H_0^2} - \left(\frac{U_{0z}^2}{U_0^2}\right)_z \\ &= -\Phi_0\frac{U_1}{H_0} + \frac{\Phi_0U_0H_1}{H_0^2} + \frac{U_0H_{1z}}{H_0^2} + 2\frac{U_{0z}}{H_0}. \end{aligned}$$

Therefore we have

$$I_1 = -\int_0^\infty \Phi_0 L_0\hat{U}_{1z}\, dz + \int_0^\infty \frac{\Phi_0U_0H_{1z}}{H_0^2}\, dz + 2\int_0^\infty \frac{\Phi_0U_{0z}}{H_0}\, dz.$$

Integrating by parts, we get

$$\int_0^\infty \Phi_0 L_0\hat{U}_{1z}\, dz = \Phi_0(\infty)\hat{U}_{1zz}(\infty).$$

Note that $U_0 \to 0$, $\Phi_0 \to -\sqrt{\eta}$ as $z \to \infty$ and using (73) we obtain

$$\hat{U}_{1zz}(\infty) = 1 - \eta$$

so that

$$\int_0^\infty \Phi_0 L_0\hat{U}_{1z}\, dz = -\sqrt{\eta} + \eta^{3/2}.$$

Next we compute

$$\int_0^\infty \frac{\Phi_0U_0H_{1z}}{H_0^2}\, dz = \frac{1}{H_0^2}\int_0^\infty U_{0z}H_{1z}\, dz = -\frac{1}{H_0^2}\int_0^\infty U_0H_{1zz}\, dz.$$

Note that H satisfies

$$0 = DH_{xx} - H + u^r\alpha^{-r}$$

so that

$$DH_{1zz}(z) \sim -\alpha^{1-r}U_0^r(z)$$

and

$$\int_0^\infty \frac{\Phi_0U_0H_{1z}}{H_0^2}\, dz \sim \frac{\alpha^{1-r}}{DH_0^2}\int_0^\infty U_0^{r+1}\, dz.$$

Finally,

$$2\int_0^\infty \frac{\Phi_0 U_{0z}}{H_0}\,dz = \frac{2}{H_0}\int_0^\infty \frac{U_{0z}^2}{U_0}\,dz = \frac{2}{3}\eta^{3/2}\int_0^\infty \frac{(w_y(y))^2}{w(y)}dy = \frac{2}{3}\eta^{3/2}.$$

In summary, we obtain

$$I_1 = \sqrt{\eta} - \frac{1}{3}\eta^{3/2} + \frac{\alpha^{1-r}}{DH_0^2}\int_0^\infty U_0^{r+1}\,dz.$$

Now

$$I_2 = \int_0^\infty \frac{U_0\Phi_0^2}{H_0}\,dz = \frac{1}{3}\eta^{3/2}$$

and finally, we write

$$I_3 = \int U_0 \frac{\Psi_{0z}}{H_0^2}\,dz.$$

Now we have

$$\frac{D\Psi_{0zz}}{\alpha^2} - \Psi_0 + r\alpha^{-r-1}U_0^r\frac{U_{0z}}{U_0} = 0$$

so that

$$\Psi_{0z} \sim -\frac{\alpha^{1-r}}{D}U_0^r;$$
$$I_3 \sim -\frac{\alpha^{1-r}}{DH_0^2}\int_{-\infty}^\infty U_0^{r+1}\,dz.$$

Therefore, we finally obtain

$$\text{rhs}(70) = \alpha\sqrt{\eta}.$$

Combining this result with (71) and recalling that $\eta = \tanh^2 L$ (Theorem 1) yields (67). Note that $\text{lhs}(67)|_{\lambda=0} = \tanh^2 L < 1$; on the other hand $\text{lhs}(67) \to \infty$ as $\lambda \to \infty$. This shows that (67) admits a positive eigenvalue. ■

We now verify Theorem 7, by solving the full eigenvalue problem (22a, 22b, 26) numerically. The numerical algorithm consists of re-formulating the eigenvalue problem as a boundary value problem, by adjoining an extra equation $\frac{d}{dx}\lambda(x) = 0$ along with an extra boundary condition $\phi_x(0) = 1$. The inner approximation (69) was used as an initial guess. We then compare the resulting λ_{numeric} with $\lambda_{\text{asymptotic}}$, obtained by solving numerically the algebraic equation (67). Using $r = 2$, $D = 1, L = 1$ and with $p = 90$ or $p = 180$ we obtain:

$$p = 90: \quad \lambda_{\text{numeric}} = 1.21197, \quad \lambda_{\text{asymptotic}} = 1.13769; \quad \text{error} = 6.5\%$$
$$p = 180: \quad \lambda_{\text{numeric}} = 1.1729, \quad \lambda_{\text{asymptotic}} = 1.13769; \quad \text{error} = 3.4\%.$$

These data indicate that doubling p halves the error. This provides a good numerical verification of Theorem 7.

6. Proof of Theorem 2

We now complete the proof of Theorem 2. First, consider the case of a single boundary spike. In this case, the eigenfunction satisfies the boundary condition (25). The corresponding eigenvalue problem is given by (29); this is equivalent to (32) with $\gamma = \frac{r}{3}\frac{1}{\int_{-\infty}^{\infty} w^r\,dy}$. But since we take $r > 1$, we have $\gamma > \gamma_0$ where γ_0 is given by (33); hence $\mathrm{Re}(\lambda) \le -c_0 < 0$ by Theorem 4. This proves the stability of a single boundary spike.

Next, consider the case of an interior spike centered at the origin. It admits two eigenvalues with corresponding eigenfunctions satisfying the boundary conditions given by (25) or (26), respectively. The former is stable as just shown. However the latter (small eigenvalue) is *always unstable*, as proven in Theorem 7.

Finally, we consider the double boundary spike case. This admits two eigenvalues. The first corresponding eigenfunction has boundary conditions (25) while the second eigenfunction satisfies boundary conditions (27). The former is stable as just shown. The latter leads to the nonlocal eigenvalue problem (30) as derived in Section 4. It follows from Theorem 3 that the corresponding eigenvalue is unstable if $r\tanh^2\left(\frac{L}{\sqrt{D}}\right) < 1$ and is stable if $r = 2$ and $r\tanh^2\left(\frac{L}{\sqrt{D}}\right) > 1$. The threshold is given by $D = D_c$ where D_c is given by (14). This completes the proof of Theorem 2.

7. Discussion

In this paper we have studied the Gierer-Meinhardt system with large reaction rates. Formal asymptotics were used to construct the steady state solutions; their stability was analyzed using a combination of formal computations and rigorous analysis. The main result, Theorem 2, is the classification of the stability of interior and boundary spike solutions. The behavior of the system differs significantly from the "standard" GM system (1). In particular, an interior spike is *unstable* with respect to translation instabilities, and moves towards the boundary. This is phenomenologically similar to the shadow GM system [18]. In contrast, the interior spike of the standard GM system is stable [7], [20]. Therefore we expect that as the nonlinearity strength p is increased, the interior spike can be destabilized. It is an open question to determine this instability threshold.

In agreement with the GM system and the shadow GM system, then single boundary spike is single. In contrast to the shadow GM system and in agreement with the GM system, the double boundary spike can be stable or unstable depending on the value of the diffusion constant of the inhibitor.

To summarize the stability results, we observe a new and interesting mixture of properties from the GM system and the shadow GM system.

In Theorem 3 we proved the stability of the large eigenvalue for a single spike under the assumption that $r = 2$. We also conjecture that the theorem remains true for any $r > 1$. It is an open question to prove this conjecture.

In our analysis, we assumed that the inhibitor has infinitely fast response ($\tau = 0$). We expect that our analysis can be extended to the case of τ small enough without too much extra effort. On the other hand, it is known that for sufficiently slow response rates (large τ), the spikes in the usual GM model can exhibit oscillatory instability due to a Hopf bifurcation in the large eigenvalue (see [19]). We believe that this is true also for the case of large reaction rates. However, the precise analysis of this bifurcation as well as the critical scaling of τ in the case of large reaction rates is an open question.

We have shown that large reaction rates are able to create spiky patterns for the GM system in a similar way as has been shown before for small diffusion constant of the activator. In this sense, large reaction rates increase the potential of the system for pattern formation. This effect corresponds well to results in [5], where it is shown that Turing instability is possible for large reaction rates, even if the diffusion constants are very close to each other.

Biologically, this is important, as it widens the range of possible applications for Turing systems to explain pattern formation into areas where there is no good justification for vastly different reaction rates but it is known that there are large reaction rates. If there is a high degree of cooperativity between the components, which is often the case for many gene hierarchies, a large reaction rate can often be explained theoretically and measured experimentally, thus opening the door for suitable Turing systems to explain the patterns observed.

8. Acknowledgements

We thank the anonymous referees. Their insightful comments and questions helped to strengthen the paper significantly. The work of JW is supported by an Earmarked Grant of RGC of Hong Kong. TK is supported by an NSERC discovery grant, Canada. MW and TK would like to thank the Department of Mathematics at CUHK for their kind hospitality, where a part of this paper was written.

References

[1] N.E. Buchler, U. Gerland, and T. Hwa, Nonlinear protein degradation on the functions of genetic circuits. *PNAS* 102 (2005), 9559-9564.
[2] A. Doelman, R. A. Gardner, and T. J. Kaper, Stability analysis of singular patterns in the 1D Gray-Scott model: a matched asymptotics approach, *Phys. D* 122 (1998), 1-36.
[3] A. Doelman, R. A. Gardner, and T. J. Kaper, Large stable pulse solutions in reaction-diffusion equations, *Indiana Univ. Math. J.* 50 (2001), 443-507.
[4] A. Gierer and H. Meinhardt, A theory of biological pattern formation, *Kybernetik (Berlin)* 12 (1972), 30-39.
[5] A. Hunding and R. Engelhardt, Early biological morphogenesis and nonlinear dynamics, *J. Theor. Biol.* 173 (1995), 401-413.
[6] P. W. Ingham, The molecular genetics of embryonic pattern formation in *Drosophila*, *Nature* 335 (1988), 25-34.
[7] D. Iron, M. J. Ward, and J. Wei, The stability of spike solutions to the one-dimensional Gierer-Meinhardt model, *Phys. D* 50 (2001), 25–62.
[8] H. Meinhardt, Models of biological pattern formation, Academic Press, London, 1982.
[9] H. Meinhardt, The algorithmic beauty of sea shells, Springer, Berlin, Heidelberg, 2nd edition, 1998.
[10] J. Murray, *Mathematical Biology, II: Spatial models and Biomedical Applications*, 3rd Edition, Springer-Verlag.
[11] C. Nüsslein-Volhard, Determination of the embryonic axes of *Drosophila*, *Development* (Suppl.) 1 (1991), 1-10.
[12] M. J. Pankratz and H. Jäckle, Making stripes in the *Drosophila* embryo, *Trends Genet.* 6 (1990), 287-292.

[13] G. Riddihough, Homing in on the homeobox, *Nature* 357 (1992), 643-644.
[14] L. J. Slater, Confluent Hypergeometric Functions, *Cambridge University Press*, 1960.
[15] I. Takagi, Point-condensation for a reaction-diffusion system, *J. Differential Equations* 61 (1986), 208-249.
[16] A. M. Turing, The chemical basis of morphogenesis, *Phil. Trans. Roy. Soc. Lond. B* 237 (1952), 37-72.
[17] N. V. Valeyev, D. G. Bates, P. Heslop-Harrison, I. Postlethwaite, and N. V. Kotov, Elucidating the mechanisms of cooperative calcium-calmodulin interactions: a structural systems biology approach, *BioMed Central Sys. Biol.* 2 (2008), 48.
[18] J. Wei, On single interior spike solutions of Gierer-Meinhardt system: uniqueness and spectrum estimates, *Eur. J. Appl. Math.* 10 (1999), 353-378.
[19] M. J. Ward and J. Wei, Hopf bifurcation of spike solutions for the shadow Gierer-Meinhardt system, *Eur. J. Appl. Math.* 14 (2003) 677-711.
[20] J. Wei and M. Winter, Existence, classification and stablity analyisis of multiple-peaked solutions for the Gierer-Meinhardt system in R^1, *Methods Appl. Anal.* 14 (2007), 119-164.
[21] J. D. Weiss, The Hill equation revisited: uses and misuses, *The FASEB Journal* 11 (1997), 835-841.
[22] D. G. Wilkinson, Molecular mechanisms of segmental patterning in the vertebrate hindbrain and neural crest, *BioEssays* 15 (1993), 499-505.

Department of Mathematics and Statistics, Dalhousie University, Halifax, Canada
E-mail address: tkolokol@mathstat.dal.ca

Department of Mathematics, The Chinese University of Hong Kong, Shatin, Hong Kong
E-mail address: wei@math.cuhk.edu.hk

Department of Mathematical Sciences, Brunel University, Uxbridge UB8 3PH, United Kingdom
E-mail address: matthias.winter@brunel.ac.uk, phone +441895267179, fax +441895269732, corresponding author